Available online at www.sciencedirect.com
SCIENCE DIRECT
Polymer 47 (2006) 5973–5978
polymer
www.elsevier.com/locate/polymer

Motional coherency in chain dynamics of polybutadiene studied by molecular dynamics simulations

Kazuhiro Takemura [a], Hidemine Furuya [a,*], Toshiji Kanaya [b]

[a] Department of Organic and Polymeric Materials, Tokyo Institute of Technology, 2-12-1-H-128 Ookayama, Meguro-ku, Tokyo 152-8552, Japan
[b] Institute for Chemical Research, Kyoto University, Uji, Kyoto 611-0011, Japan

Received 28 February 2006; received in revised form 2 June 2006; accepted 2 June 2006
Available online 23 June 2006

Abstract

Molecular dynamics simulations of 1,4-polybutadiene in bulk amorphous state were performed. Results were compared with the recent neutron spin-echo measurements. To investigate motional coherency the relaxation rates for the collective and self-motions, the collective and self-relaxation rates, were evaluated for the short and long time regimes of the normalized intermediate scattering functions. The scattering vector dependence of the collective relaxation rates estimated for both fast and slow processes indicated a minimum at scattering vector $q = 1.5$ Å^{-1}, corresponding to the position of a peak in the static structure factor. The self-relaxation rates increased monotonously with q. A phenomenon known as de Gennes narrowing was reproduced well in the simulation and found to be originated from the inter-molecular correlation. The collective relaxation rate evaluated for fast process appeared to modulate around a peak of $q = 2.9$ Å^{-1}, corresponding to the intra-molecular correlation.

Keywords: Polybutadiene; Molecular dynamics simulation; de Gennes narrowing

1. Introduction

Many studies have investigated the dynamics of amorphous materials at the glass transition. As the glass transition approached, molecules become localized and relaxation times increase by many orders of magnitude indicating a broad distribution [1]. Cooperative motion is one of the keys to understand the dynamical behavior near the glass transition temperature (T_g). Motional coherency can be examined by coherent neutron scattering techniques [2]. The relation between coherent neutron scattering and one of the diffraction peaks in the X-ray pattern was theoretically deduced by de Gennes [3] and phenomenological approaches generalize the de Gennes narrowing [4,5]. The de Gennes narrowing has been observed in materials such as polybutadiene (PB) [6], polyisobutylene [7], polyisoprene [8] and polystyrene [9] star polymer, propylene glycol [10], and neopentane [11]. The de Gennes narrowing is usually observed for motional slowing down at the peak in the structure factor due to inter-molecular coherency arising as a consequence of molecular packing. Richter et al. have presented neutron spin-echo data of polybutadiene [6] and found that the estimated relaxation rate passes through a broad minimum at about $q = 1.5$ Å^{-1}. Peaks at $q = 1.5$ and 2.9 Å^{-1} have been observed in the static structure factor $S(q)$ of PB [12,13], which suggest the relaxation rate might indicate minimum at both $q = 1.5$ and 2.9 Å^{-1} due to the de Gennes prediction. Recently, a neutron spin-echo study [13], in which the q range was extended up to 3.5 Å^{-1}, has been performed on deuterated PB near T_g. The evaluated relaxation rate indicates no minimum at around $q = 2.9$ Å^{-1}. These observed results need to be investigated on atomic level.

Molecular dynamics (MD) simulation is one of the most promising methods to figure out the detail of molecular motion. Many MD calculations have been performed on bulk

* Corresponding author. Tel./fax: +81 3 5734 2806.
E-mail address: hfuruya@polymer.titech.ac.jp (H. Furuya).

0032-3861/$ - see front matter © 2006 Elsevier Ltd. All rights reserved.
doi:10.1016/j.polymer.2006.06.004

amorphous PB [14–23]. Gee and Boyd have performed the MD simulations of PB to analyze conformational dynamics [14]. Smith et al. carried out the MD simulations of PB melt to investigate chain dynamics and compare them with NMR, dielectric relaxation, and neutron spin-echo measurements [15–17]. Recently Okada et al. have employed the MD calculations of *cis*-1,4-PB to elucidate the origin of a fast relaxation process observed by quasielastic neutron scattering [18,19]. The more recent MD work of Tsolou et al. investigated the dynamic properties of *cis*-1,4-PB systems, ranging in molecular length from 32 to 400 carbons. Chain length dependence of self-diffusion coefficient and friction coefficient was calculated in detail and a departure from predictions of the Rouse model toward a reptation-like behavior was observed [23].

Studies related to the de Gennes narrowing by MD simulations were reported. Neelakantan and Maranas have investigated the relaxation times of four hydrocarbon polymers by MD simulations and reported that the modulation of the relaxation times near the peak in the static structure factor was observed and qualitatively described by the narrowing picture suggested by de Gennes [24,25]. However, their studies have been related to intermediate scale for q below 2.9 Å^{-1}.

In this study, we performed MD simulations of PB molecules in bulk amorphous phase. Molecular motion and motional coherency were investigated by intermediate scattering functions to compare with the recent neutron spin-echo study for wide q range [13].

2. Method of MD simulation

All the MD calculations were performed using the Discover3/InsightII 400P (Accelrys Inc.) with the COMPASS force field. All atom models of four PB molecules consisting of 50 monomer units and their periodic images are contained in a cubic MD cell. The chains are random copolymers of 47% 1,4-*cis*, 46% 1,4-*trans*, and 7% 1,2-vinyl units. The length and the configuration of the chains are same as those of the samples used for the recent neutron scattering measurements. The temperature of the system was set at 400 K for the initial equilibration. The density of the system at 400 K was also set at the observed density for the initial state. The temperature was lowered gradually down to 10 K. The equilibration runs at each temperature were performed for at least 2 ns under constant temperature and constant pressure. Temperature was controlled using velocity scaling method and pressure was controlled using Berendesen method [26]. The pressure of the MD system was kept at 0.1 MPa. The sampling runs at each temperature were carried out under constant temperature and constant volume. The duration of the sampling run was over 10 ns. Especially, the duration of the sampling runs at 200–250 K near the glass transition temperature was 20–100 ns. Several sampling runs at same temperature were carried out to improve the averaged values of analyzed results. The method proposed by Nosé and Hoover [27,28] to control temperature was employed for the sampling runs. For the numerical integration of the Newtonian equation of motion, time step of 1 fs and 0.25 fs were chosen for the equilibration runs and the sampling runs, respectively. A cut-off radius of 12 Å for the van der Waals potential and for the electrostatic interactions was used.

3. Results and discussion

The temperature of the system was set at 400 K for the initial equilibration and gradually decreased after the system was confirmed to be in the equilibrium state by checking the change of the density at each temperature. The temperature dependence of the specific volume is shown in Fig. 1. The values of the density obtained from the simulation are in agreement with the experimental data within the error of about 5%. The estimated coefficient of thermal expansion at 300 K was $7.6 \times 10^{-4}\ \text{K}^{-1}$. This value is similar to the previous MD result [18] of $5.2 \times 10^{-4}\ \text{K}^{-1}$ for *cis*-1,4-PB and the dilatometric result [29] of $6.7 \times 10^{-4}\ \text{K}^{-1}$ for PB with 55% 1,4-*cis* content. The intersection of the two lines fitted to the plots for the high and low temperature regions at about 170 K corresponds to the glass transition temperature, which is in agreement with the experimental value of 180 K for copolymer of 1,4-*cis*, 1,4-*trans*, and 1,2-vinyl PB [12,13].

In order to investigate the static structure of the bulk amorphous phase, the coherent scattering differential cross section $(\mathrm{d}\sigma/\mathrm{d}\Omega)_{\mathrm{coh}}$ was calculated by [30]

$$(\mathrm{d}\sigma/\mathrm{d}\Omega)_{\mathrm{coh}} = \sum_i \chi_i \sum_j b_i b_j \left\{ \delta_{ij} + \langle \rho_j \rangle \int 4\pi r^2 \left[g_{ij}(r) - 1 \right] \times \frac{\sin qr}{qr} \mathrm{d}r \right\} \quad (1)$$

where b_i is the neutron scattering length of atom i and χ_i is the atomic fraction of the atom i. The pair distribution function $g_{ij}(r)$ is given by

$$g_{ij}(r) = \rho_{ij}(r)/\langle \rho_j \rangle \quad (2)$$

where ρ_{ij} is the density of atom j at a distance r from an atom i in the system, $\langle \rho_j \rangle$ is the average density of atom j. The calculated $(\mathrm{d}\sigma/\mathrm{d}\Omega)_{\mathrm{coh}}$ at 200 K is shown in Fig. 2, where a sharp peak at $q = 1.5\ \text{Å}^{-1}$ and a broad peak at $q = 2.9\ \text{Å}^{-1}$

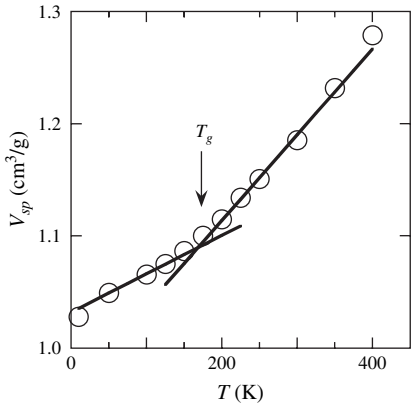

Fig. 1. Temperature dependence of the specific volume obtained from MD simulation. Intersection indicates glass transition temperature.

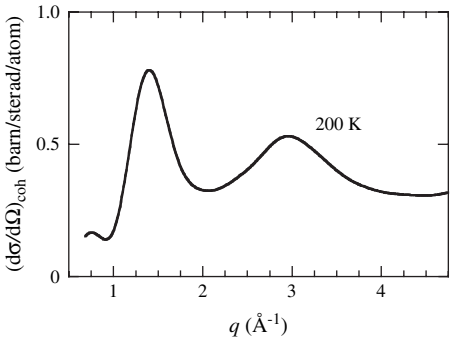

Fig. 2. Coherent scattering differential cross section of perdeuterated PB calculated from MD simulation at 200 K.

are observed. The peak positions of the calculated pattern are in good agreement with the data observed by wide-angle neutron scattering measurements [12,13,23]. The calculated results for the static structure and thermal properties indicated that the system in the simulation was considered to be similar to the real system of the polymer used by the experiments. To estimate the relations of intra- and inter-molecular correlations with the peaks observed in Fig. 2, the pair distribution functions of intra- and inter-molecular pairs were calculated. According to the method of Furuya et al. [30] a pair between monomers i and j in the same molecules was regarded as an intra-molecular pair only if the monomer index difference, $m \equiv |i-j|$, is equal to 5 or smaller. Fig. 3a shows the calculated pair distribution functions. The thick dotted line is for the intra-molecular pairs and the thin solid line for the inter-molecular pairs. At small r, much fine structure is seen in the intra-molecular function, but the inter-molecular function is practically zero for r below about 3 Å. These results indicate that the peak at $q = 2.9$ Å^{-1} in Fig. 2 originates from the intra-molecular correlations. As r increases, the inter-molecular pair distribution function approaches the constant value for r above 4 Å, whereas the intra-molecular function gradually diminishes toward zero. Fig. 3b shows the pair distribution function of inter- and intra-molecular vinyl carbon C* pairs indicating in the inset. The pair distribution function for the first neighbor vinyl carbon C* pairs ($m = 1$) shows peaks for $r = 4$ and 5 Å, and the inter-molecular function is practically zero for r below 4 Å. According to the functions, the inter-monomer distance and the inter-chain distance are between 4 and 5 Å. These results suggest that the peak at $q = 1.5$ Å^{-1} in Fig. 2 is attributed to both inter- and intra-molecular correlations. Since the inter-molecular function at $r = 4.2$ Å ($= 2\pi/1.5$ Å^{-1}) is larger than the intra-molecular function in Fig. 3a, the peak at $q = 1.5$ Å^{-1} is found to be mainly attributed to inter-molecular correlation.

To investigate chain mobility and to compare with results of neutron spin-echo measurements, the intermediate scattering functions were evaluated. The intermediate scattering functions provide information regarding self and collective motions of atoms or molecules. We estimate the self- and collective intermediate scattering functions. The observable in a coherent neutron spin-echo experiment is directly related to the collective intermediate scattering function, $I(q,t)$.

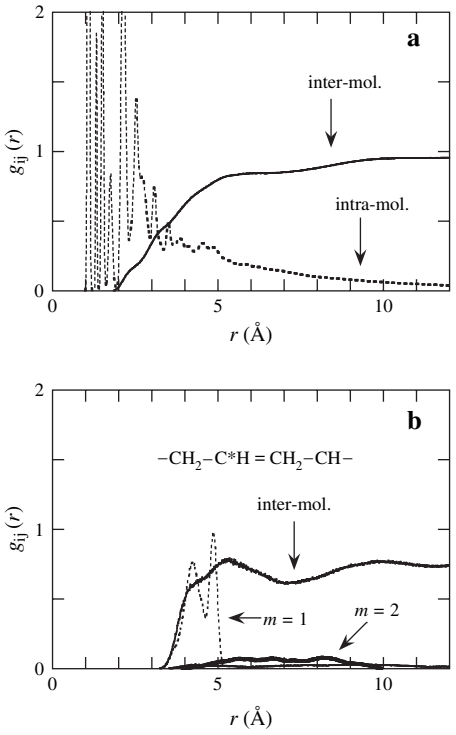

Fig. 3. (a) Pair distribution functions of all atoms for intra- and inter-molecular pairs; (b) Pair distribution functions of a vinyl carbon (C*) for intra- and inter-molecular pairs where m denotes monomer index difference.

The collective intermediate scattering function $I(q,t)$ including self- and distinct-parts and the self-intermediate scattering function $I_s(q,t)$ were calculated by the method of Chang and Yethiraj [31]. The intermediate scattering functions $I(q,t)$ and $I_s(q,t)$ are estimated starting with the van Hove correlation function $G(r,t)$ and $G_s(r,t)$ [32],

$$G(r,t) = \frac{1}{N}\left\langle \sum_{i=1}^{N}\sum_{j=1}^{N} \delta[r + r_j(0) - r_i(t)] \right\rangle \tag{3}$$

$$G_s(r,t) = \frac{1}{N}\left\langle \sum_{i=1}^{N} \delta[r + r_i(0) - r_i(t)] \right\rangle \tag{4}$$

where N is the total number of atoms in the system and $r_i(t)$ is the position of atom i at time t. We also carried out the extension of the method of Salacuse et al. [33] as Chang and Yethiraj performed. Since $G(r,t)$ approaches the total density $\rho = N/V$ (V is the volume) and $G_s(r,t)$ approaches $1/V$ as r increases, ρ is subtracted from $G(r,t)$ when calculating $I(q,t)$, i.e.,

$$I(q,t) = 4\pi \int r^2 \frac{\sin qr}{qr}[G(r,t) - \rho]\mathrm{d}r \tag{5}$$

$$I_s(q,t) = 4\pi \int r^2 \frac{\sin qr}{qr}[G_s(r,t) - 1/V]\mathrm{d}r \tag{6}$$

where the isotropic condition was used.

The normalized collective and self-intermediate scattering functions, denoted by $I(q,t)/I(q,0)$ and $I_s(q,t)/I_s(q,0)$, for several

scattering vectors q at 200, 225 and 250 K are shown in Fig. 4. The characteristics of the calculated intermediate scattering function curves are similar to the results of other MD simulations [18,22,23]. Two regimes which correspond to the fast and slow motions can be observed before and after the crossover of these regimes at $t = 1$ ps. The relaxation for $t < 1$ ps was defined as fast process, while the relaxation for $t > 1$ ps was defined as slow process. For long length scale, $q = 1.2$ and 1.8 Å^{-1}, $I_s(q,t)/I_s(q,0)$ decays faster than $I(q,t)/I(q,0)$. While for $q = 2.2$, 2.9, and 3.4 Å^{-1}, $I_s(q,t)/I_s(q,0)$ and $I(q,t)/I(q,0)$ are almost same. These results indicate that PB molecules move randomly on short length scale, while cooperatively on inter-chain and inter-monomer length scale. As with previous neutron scattering studies, the overall decay may be described by a two-step function: single exponential function $(A\exp[-(t/\tau_f)])$ for a fast process and a stretched exponential function $(A\exp[-(t/\tau)^{\beta}]$, $0 < \beta < 1.0)$ for a slow process. The relaxation time τ_f and τ characterize the fast and slow processes, and β is the stretching parameter. The values of normalized intermediate scattering functions in the range of 5 to 500 ps were fitted with the stretched exponential function, while the single exponential function was used to fit normalized intermediate scattering functions in the range of 0.005 to 0.1 ps. Fig. 5 illustrated the fitting results of the normalized collective intermediate scattering functions for $q = 1.2$, 2.2, and 3.2 Å^{-1} at 200 K. Values of the stretched parameter β for the best fits were around 0.35. It is evident that the overall decay of the intermediate scattering functions can be described by the sum of two exponential functions.

The relaxation rates for collective and self-motion, $\Gamma(q)$ and $\Gamma_s(q)$, (or inverse of the relaxation times $\tau(q)^{-1}$), which are termed as the collective and self-relaxation rates, were obtained from the results of fits for the slow processes of $I(q,t)/I(q,0)$ and $I_s(q,t)/I_s(q,0)$, respectively. Fig. 6 shows the scattering vector dependence of the relaxation rates $\Gamma(q)$ and $\Gamma_s(q)$ at 200, 225, and 250 K. For q above 2.0 Å^{-1}, $\Gamma(q)$ and $\Gamma_s(q)$ are identical and increase as q increases. For q below 2.0 Å^{-1}, $\Gamma_s(q)$ monotonously increases with increasing q, whereas $\Gamma(q)$ exhibits a minimum at 1.2 Å^{-1}. When temperature increases, the values of the relaxation rates $\Gamma(q)$ and $\Gamma_s(q)$ increase. In Fig. 7, the relaxation rates $\Gamma(q)$ and $\Gamma_s(q)$ are

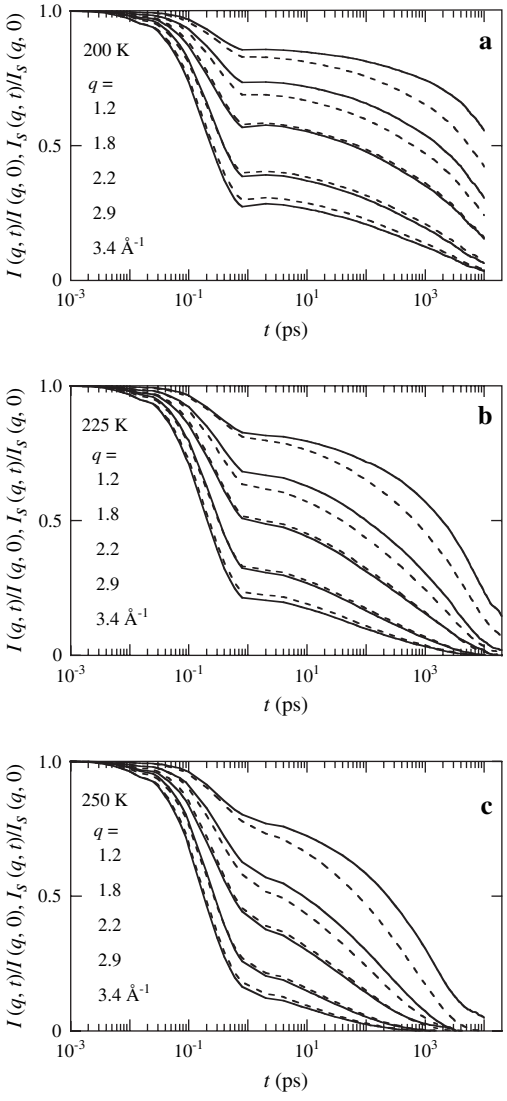

Fig. 4. Normalized intermediate scattering functions for several scattering vectors at (a) 200 K, (b) 225 K, and (c) 250 K. Solid lines are collective intermediate scattering functions $I(q,t)/I(q,0)$ including self- and distinct-part. Broken lines are self-part of intermediate scattering functions $I_s(q,t)/I_s(q,0)$.

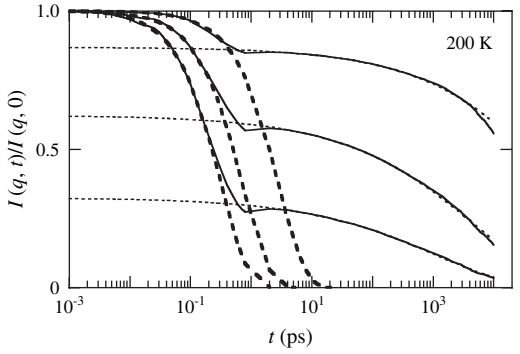

Fig. 5. Collective intermediate scattering functions $I(q,t)/I(q,0)$ for $q = 1.2$, 2.2 and 3.4 Å^{-1} at 200 K. Thin dotted lines are the results of the KWW function fits to the data for t between 5 and 500 ps. Thick broken lines are the results of the exponential fits to the data for t between 0.005 and 0.1 ps.

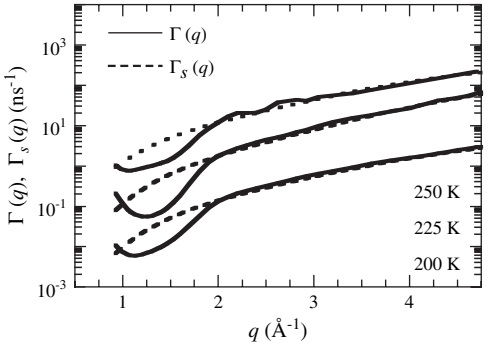

Fig. 6. Scattering vector dependence of the relaxation rates, $\Gamma(q)$ and $\Gamma_s(q)$, for slow process at 200, 225 and 250 K. Solid lines are collective relaxation rates estimated from normalized intermediate scattering functions $I(q,t)/I(q,0)$ including self and distinct-parts. Dotted lines indicate self-relaxation rates estimated from self-intermediate scattering functions $I_s(q,t)/I_s(q,0)$.

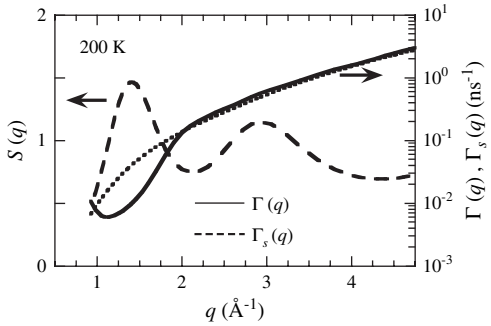

Fig. 7. Comparison between static structure factor (broken line) and collective (solid line) and self (dotted line) relaxation rates.

compared with the calculated static structure factor $S(q)$ ($=I(q,0)$) at 200 K. It is obvious that the minimum of $\Gamma(q)$ correlates with the peak at 1.5 Å^{-1} observed in $S(q)$, a result which qualitatively could be understood in terms of the so-called de Gennes narrowing, while $\Gamma(q)$ monotonously increases with q in the region observed a peak at 2.9 Å^{-1} in $S(q)$. The de Gennes narrowing is not observed at around the second peak ($q = 2.9$ Å^{-1}) of $S(q)$. These results support the observation of the recent neutron spin-echo study [13].

In order to evaluate the spatial dependence of the observed $\Gamma(q)$ and $\Gamma_s(q)$ in terms of molecular correlations, the normalized collective and self-intermediate scattering functions were separated into the contribution of the intra- and inter-molecular pairs. The relaxation rates $\Gamma(q)$ and $\Gamma_s(q)$ for the intra- and inter-molecular pairs were obtained by the fitting analysis of the normalized intermediated scattering functions for the intra- and inter-molecular pairs, respectively. Fig. 8a and b shows the relaxation rates for the intra- and inter-molecular pairs at 200 K, respectively. In Fig. 8a, $\Gamma(q)$ and $\Gamma_s(q)$ for the intra-molecular pairs monotonously increase with q. For the inter-molecular pairs, $\Gamma(q)$ passes through minimum at 1.5 Å^{-1}, while $\Gamma_s(q)$ increases with increasing q as well as the intra-molecular pairs. The static structure factors $S(q)$ at 200 K for the inter- and intra-molecular pairs are also plotted in Fig. 8a and b. A peak at 2.9 Å^{-1} is observed for intra-molecular pairs. The thick broken line is for inter-molecular pairs and indicates a peak at 1.5 Å^{-1}. These results indicate that the minimum of $\Gamma(q)$ is attributed to inter-molecular correlation. The collective motion of slow relaxation process are slowed down at $q = 1.5$ Å^{-1} where there is a peak in the inter-molecular static structure factor.

Fig. 9 shows the scattering vector dependence of collective and self-relaxation rates, $\Gamma^{\text{f}}(q)$ and $\Gamma_{\text{s}}^{\text{f}}(q)$, for collective and self-motions of fast process comparing with $S(q)$. There exist differences between $\Gamma^{\text{f}}(q)$ and $\Gamma_{\text{s}}^{\text{f}}(q)$ for all q observed. The self-relaxation rate $\Gamma_{\text{s}}^{\text{f}}(q)$ for fast process monotonously increases with q as well as the rate for slow process, $\Gamma_{\text{s}}(q)$. The collective relaxation rate, $\Gamma^{\text{f}}(q)$, passes through a minimum around 1.2 Å^{-1}. The trend of $\Gamma^{\text{f}}(q)$ below 2 Å^{-1} was found to be similar to the rate $\Gamma(q)$ for slow process. The value of $\Gamma^{\text{f}}(q)$ above 2 Å^{-1} appeared to modulate at 2.9 Å^{-1} corresponding to the intra-molecular correlation. For short time regime ranging from 0.005 ps to 0.1 ps, the collective motion is

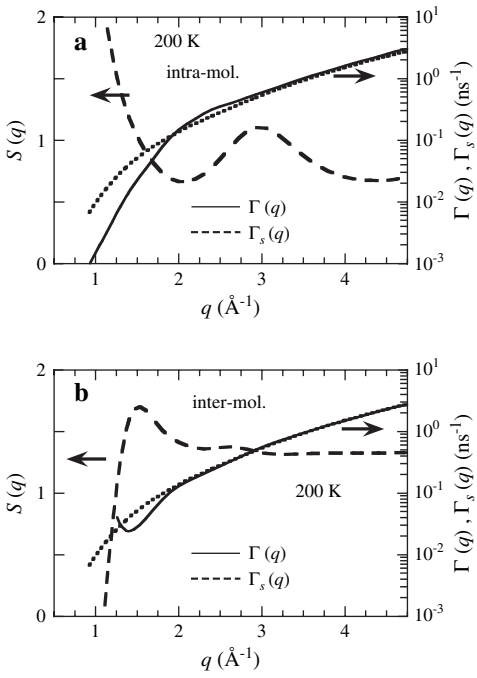

Fig. 8. Collective (solid line) and self (dotted line) relaxation rates for slow process: (a) intra-molecular pairs and (b) inter-molecular pairs. Broken lines give static structure factors for (a) intra- and (b) inter-molecular pairs.

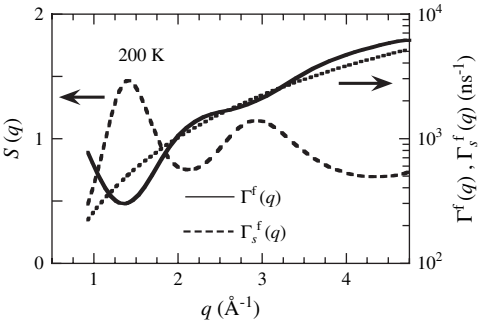

Fig. 9. Collective (solid line) and self (dotted line) relaxation rates, $\Gamma^{\text{f}}(q)$ and $\Gamma_{\text{s}}^{\text{f}}(q)$, for fast process at 200 K. Static structure factor (broken line) is given for comparison.

found to be different from self-motion and much sensitive to spatial correlations, inter and intra-molecular correlations. The relaxation rates obtained for the long time regime of intermediate scattering function seems to be insensitive to short distance correlation in high q range of $S(q)$ because of time scale analyzed.

4. Conclusion

We performed molecular dynamics simulations of 1,4-polybutadiene in bulk amorphous state. The calculated static properties such as the glass transition temperature, coefficient of thermal expansion, and coherent scattering differential cross section are in good agreement with experiments. Peaks at scattering vector $q = 1.5$ and 2.9 Å^{-1} are observed in the static structure factor and attributed to inter- and intra-molecular

correlation, respectively. To investigate motional coherency the relaxation rates were estimated for the short and long time regimes of the normalized intermediate scattering functions. The collective relaxation rates, $\Gamma^{f}(q)$ and $\Gamma(q)$, for both fast and slow relaxation processes pass through minimum at $q = 1.2$ Å^{-1}, corresponding to the position of the peak in the static structure factor, a phenomenon known as de Gennes narrowing. The self-relaxation rate $\Gamma_{s}(q)$ estimated for slow process shows no minimum and insensitive to the static structure factor. The self-relaxation rate $\Gamma_{s}^{f}(q)$ evaluated for fast process also shows no minimum. For q above 2.0 Å^{-1}, the collective relaxation rate $\Gamma(q)$ increases monotonously while the $\Gamma^{f}(q)$ for fast process relatively modulates and correlates to the static structure factor. The motional coherency for inter-chain correlation of PB was intensively observed and found to be a key role for the de Gennes narrowing. The collective motion for fast process was also slightly affected by the intra-chain correlation. Further investigation for details of the coherent motions and relaxation time distributions is underway and will be reported.

References

[1] Kanaya T, Tsukushi I, Kaji K, Gabrys B, Bennington SM. J Non-Cryst Solids 1998;235–237:212–8.
[2] Kanaya T, Tsukushi I, Kaji K, Gabrys BJ, Bennington SM, Furuya H. Phys Rev B 2001;64:144202-1–1442025.
[3] de Gennes PG. Physica 1959;25:825–39.
[4] Sköld K. Phys Rev Lett 1967;19:1023–5.
[5] Sköld K, Larsson KE. Phys Rev 1967;161:102–16.
[6] Richter D, Frick B, Farago B. Phys Rev Lett 1988;61:2465–8.
[7] Farago B, Arbe A, Colmenero J, Faust R, Buchenau U, Richter D. Phys Rev E 2002;65:051803-1–17.
[8] Richter D, Stühn B, Ewen B, Nerger D. Phys Rev Lett 1987;58:2462–5.
[9] Richter D, Farago B, Huang JS, Fetters LJ, Ewen B. Macromolecules 1989;22:468–72.
[10] Swenson J, Köper I, Telling MTF. J Chem Phys 2002;116:5073–9.
[11] Smorenburg HE, Crevecoeur RM, de Graaf LA, de Schepper IM. Phys Rev E 1996;54:6304–12.
[12] Arbe A, Richter D, Colmenero J, Farago B. Phys Rev E 1996;54:3853–69.
[13] Kanaya T, Kakurai K, Tsukushi I, Inoue R, Watanabe H, Nishi M, et al. J Phys Soc Jpn 2005;74:3236–40.
[14] Gee RH, Boyd RH. J Chem Phys 1994;101:8028–38.
[15] Smith GD, Paul W, Monkenbusch M, Willner L, Richter D, Qiu XH, et al. Macromolecules 1999;32:8857–65.
[16] Smith GD, Paul W, Monkenbusch M, Richter D. J Chem Phys 2001;114:4285–8.
[17] Smith GD, Borodin O, Paul W. J Chem Phys 2002;117:10350–9.
[18] Okada O, Furuya H. Polymer 2002;43:971–6.
[19] Okada O, Furuya H, Kanaya T. Polymer 2002;43:977–82.
[20] Kim EG, Mattice WL. J Chem Phys 1994;101:6242–54.
[21] Haliloğlu T, Bahar I, Erman B, Kim EG, Mattice WL. J Chem Phys 1996;104:4828–34.
[22] van Zon A, de Leeuw SW. Phys Rev E 1998;58:R4100–3.
[23] Tsolou G, Mavrantzas VG, Theodorou DN. Macromolecules 2005;38:1478–92.
[24] Neelakantan A, Maranas JK. J Chem Phys 2004;120:465–74.
[25] Neelakantan A, Maranas JK. J Chem Phys 2004;120:1617–26.
[26] Berendesen HJC, Postma JPM, van Gunsteren WF, DiNola A, Haak JR. J Chem Phys 1984;81:3684–90.
[27] Nosé SJ. Chem Phys 1984;81:511–9.
[28] Hoover WG. Phys Rev A 1985;31:1695–7.
[29] Pedemonte E, Bianchi U. Polym Lett 1964;2:1025–7.
[30] Furuya H, Mondello M, Yang HJ, Roe RJ, Erwin RW, Han CC, et al. Macromolecules 1994;27:5674–80.
[31] Chang R, Yethiraj A. J Chem Phys 2002;116:5284–98.
[32] van Hove L. Phys Rev 1954;95:249–62.
[33] Salacuse JJ, Denton AR, Egelstaff PA. Phys Rev E 1996;53:2382–9.